

Observation of a Kohn Anomaly in the Surface-Phonon Dispersion Curves of Pt(111)

U. Harten, J. Peter Toennies, Christof Wöll, and G. Zhang

Max-Planck-Institut für Strömungsforschung, 3400 Göttingen, Federal Republic of Germany

(Received 15 August 1985)

Surface-phonon dispersion curves have been measured by He-atom inelastic scattering for Pt(111) along the $\langle 1\bar{1}0 \rangle$ and $\langle 11\bar{2} \rangle$ azimuths with greatly reduced scatter compared with earlier work. Along the $\langle 1\bar{1}0 \rangle$ direction the results reveal a number of anomalous kinks in the Rayleigh-mode dispersion curve. Comparison with the corresponding anomaly in the bulk suggests that the effect is due to a two-dimensional surface Kohn anomaly.

PACS numbers: 68.30.+z, 63.20.Kr, 79.20.Nc

In metals the dielectric response $\epsilon(q)$ of the electrons, which screens the ion core movements, shows divergences in its gradient at special values of the wave vector q as a result of the existence of a well-defined Fermi surface. As first pointed out by Kohn¹ these singularities will effect the phonon dispersion curves. In the simplest case this occurs for phonons with wave vectors q given by the relationship $|\mathbf{G}_0 + \mathbf{q}| = 2k_F$, where \mathbf{G}_0 is a reciprocal-lattice vector and k_F the electron Fermi wave vector. Kohn anomalies have been observed as weak links in the dispersion curves of the bulk phonon modes in several metals such as Pd, Pb, and Pt.² These anomalies are expected to be strongly enhanced with reduced dimensionality of the Fermi surface³ and in one dimension (and at low temperatures) they have been shown to lead even to a reconstruction of the lattice (Peierls transition).⁴ Whereas their existence has been demonstrated once before in a two-dimensional layered compound,⁵ no evidence has so far been presented for a Kohn anomaly on the surface of a metal. Such an anomaly might occur via a coupling to surface electronic states. There is considerable interest in the possibility of Kohn anomalies on surfaces in connection with a mechanism for driving the often observed reconstruction of metal surfaces.⁶⁻⁸ This mechanism is also frequently referred to as a charge-density-wave instability.⁹ Previous He-atom phonon-dispersion-curve measurements on the (111) surface of Cu, Ag, and Au^{10,11} have failed to show any evidence for Kohn-type anomalies, although they do reveal a new longitudinal mode attributed to a strong 50% softening of the lateral forces in the surface layer.¹² In the present work we report on the first observation of an anomaly in the transverse surface Rayleigh dispersion curve in Pt(111) along the $\langle 1\bar{1}0 \rangle$ direction. The surface anomaly is considerably narrower than observed in the bulk along the equivalent direction and is accompanied by a strong broadening of the inelastic phonon peak. In addition, another longitudinal branch is found at higher frequencies, similar to the longitudinal mode observed in Cu, Ag, and Au.

The surface-phonon dispersion curves have been measured by use of high-resolution He-atom time-of-

flight spectroscopy. The apparatus is the same as that described previously.¹¹ A nearly monochromatic ($\Delta v/v < 1\%$) He-atom beam from a high-pressure variable-temperature (40–300 K) source (orifice 10 μm) is chopped into short bursts (3 μsec) and then scattered from the metal target in an UHV chamber ($p = 5 \times 10^{-11}$ mbar) into a direction 90° to the incident beam. The precision of the measurements, which was previously limited by a small nonreproducibility in incident angles, has been greatly improved by rotation of the target in small steps of 0.25° with a stepping motion controlled by an absolute angle coder and minicomputer, which also accumulated the data. Two Pt crystals (8 mm diameter) were prepared from a large single crystal and oriented to better than 0.3° . The final preparation in the target chamber involved Ne-ion sputtering and annealing as well as exposures to H_2 and O_2 at elevated temperatures until satisfactory LEED and Auger spectra were obtained. Carbon contamination was usually beyond the sensitivity of the cylinder-mirror Auger analyzer ($< 1\%$). For the first time on a fcc (111) surface we were able to see diffraction along the $\langle 1\bar{1}0 \rangle$ direction (10^{-4} of the specular peak) in addition to the $\langle 11\bar{2} \rangle$ direction (10^{-3} of specular peak). At low target temperatures (160 K) the target was cleaned every 2 h by flashing to 400 K.

Figure 1 shows a series of time-of-flight spectra transformed to energy-loss distributions along the $\langle 1\bar{1}0 \rangle$ direction. The Pt(111) distributions resemble those of Cu, Ag, and Au in that they show two inelastic maxima. The spectra were fitted by the least-squares method with two Gaussian distributions, and the locations of the maxima were used to determine the dispersion curves. The tail on the left, not fitted by the Gaussian distribution, is attributed to bulk phonons, while the small intensity on the right is a measure of multiphonon contributions. Neither are expected to affect the fitted peak locations and half-widths.

Figure 2 shows one of more than five sets of measurements, each consisting of about 120 time-of-flight spectra for each azimuth. The beam energy E_i in the $\langle 1\bar{1}0 \rangle$ measurements was kept fixed at 24.3 meV. The

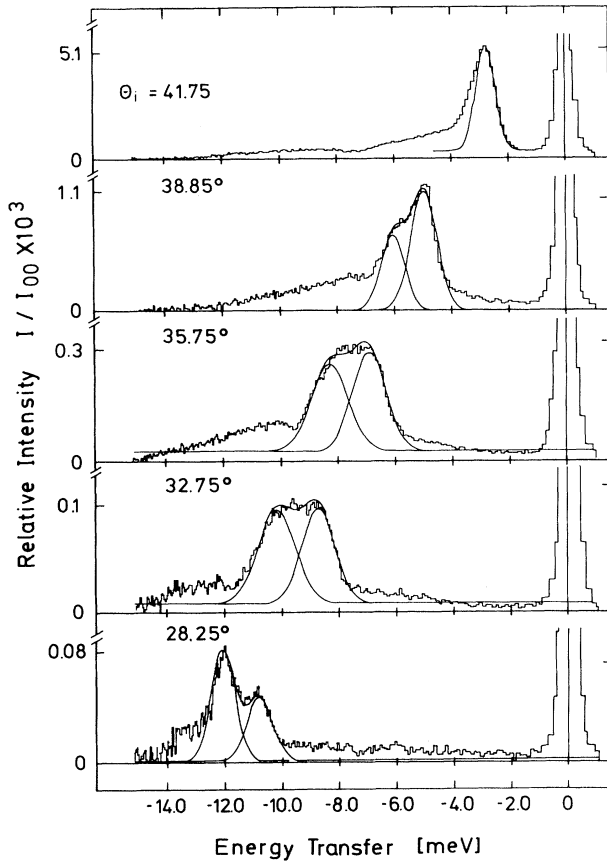


FIG. 1. Some typical measured time-of-flight spectra transformed to an energy scale for creation of phonons on Pt(111) along $\langle 1\bar{1}0 \rangle$; $E_i = 24.3$ meV and $T = 160$ K. The solid curves show best-fit Gaussian distributions. The peak at the right is due to elastic incoherent scattering.

results have been least-squares fitted by a Fourier expansion with nine coefficients, which is shown as a solid curve. The reproducibility of different sets of measurements was within the mean deviation of ≈ 0.1 meV (see below). The anomalous behavior in the lower-frequency Rayleigh dispersion curve along the $\langle 1\bar{1}0 \rangle$ direction is seen to begin at about $Q = 0.5 \text{ \AA}^{-1}$ and extends up to 1.0 \AA^{-1} , whereas along $\langle 11\bar{2} \rangle$ no anomaly is observed. The location of the second higher-frequency branch in the dispersion curve is quite similar to that observed in Cu(111) and Ag(111). The extrapolated surface-wave group velocity of 11.1 meV \AA at $Q = 0$ agrees reasonably well with the calculated value of 10.1 meV \AA based on elastic constants for $T = 0$ K.¹³

The data of Fig. 2 have been fitted by a Fourier expansion,

$$\omega_{\text{fit}}^2(Q) = \sum_{n=1}^N A_n [1 - \cos(n\pi Q/Q_{\text{max}})], \quad (1)$$

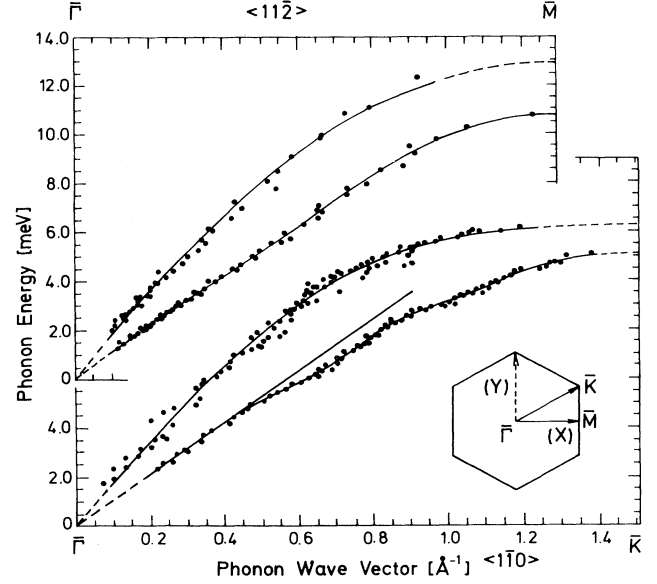


FIG. 2. Measured surface-phonon dispersion curves for Pt(111). The upper two curves are for the $\bar{\Gamma}-\bar{M}$ ($\langle 11\bar{2} \rangle$) direction and the bottom two curves for the $\bar{\Gamma}-\bar{K}$ ($\langle 1\bar{1}0 \rangle$) direction. The beam energies in both experiments were at fixed values between 10 and 32 meV. The target temperature in the $\langle 11\bar{2} \rangle$ measurements was 400 K, and in the $\langle 1\bar{1}0 \rangle$ measurements 160 K. The curves show the best-fit Fourier expansions. The solid line in the lowest set of data corresponds to a group velocity of 11.1 MeV \AA .

where Q_{max} is the wave vector at the Brillouin zone boundary, by minimalization of the mean square deviation

$$\sigma = \left[(1/M) \sum_{i=1}^M (\omega_i - \omega_{\text{fit}})^2 \right]^{1/2}.$$

The Rayleigh mode in the $\langle 1\bar{1}0 \rangle$ direction could only be fitted satisfactorily by the inclusion of nine coefficients, and the remaining root-mean-square deviation was 0.09 meV; additional Fourier terms lead to no further reduction in σ . The best-fit Fourier coefficients are summarized in Table I together with our fit of the 90-K data for the bulk, taken from Ref. 2, Table II. The extrapolated zone-boundary frequencies of 11.1 meV (\bar{K}) and 10.8 meV (\bar{M}) are to be compared with the values from a recent single-force-constant model calculation of 9.80 meV (\bar{M}) and 10.42 meV (\bar{K}), respectively.¹⁴ The same model was previously found to provide the best fit for Cu, Ag, and Au.¹¹

In order to compare the anomaly in the surface and bulk, the derivative of Eq. (1), which is the group velocity, is shown in Fig. 3(b) for the $\langle 1\bar{1}0 \rangle$ direction together with the bulk group velocity [Fig. 3(c)] for the same direction. Also shown at the top [Fig. 3(a)] are the half-widths of the Rayleigh peak obtained with

TABLE I. Fourier coefficients providing a best fit of the measured surface curves and bulk data (presented in Ref. 2).

Mode	(111) surface				Bulk [110] T_i
	$\langle 1\bar{1}0 \rangle$ Lower	$\langle 1\bar{1}0 \rangle$ Upper	$\langle 11\bar{2} \rangle$ Lower	$\langle 11\bar{2} \rangle$ Upper	
A_1	60.75	74.60	58.24	83.66	124.5
A_2	-4.808	16.15	-6.42	6.04	-18.03
A_3	1.087	...	-0.33	...	-1.157
A_4	-0.327	...	1.11	...	4.119
A_5	0.923	1.931
A_6	0.257	1.191
A_7	-1.341	0.713
A_8	0.403	0.429
A_9	0.448	0.087
σ (meV)	0.09	0.30	0.11	0.28	0.062
ω_{\max} (meV)	11.1	12.2	10.8	12.9	...
Q_{\max} (\AA^{-1})	1.51		1.31		...

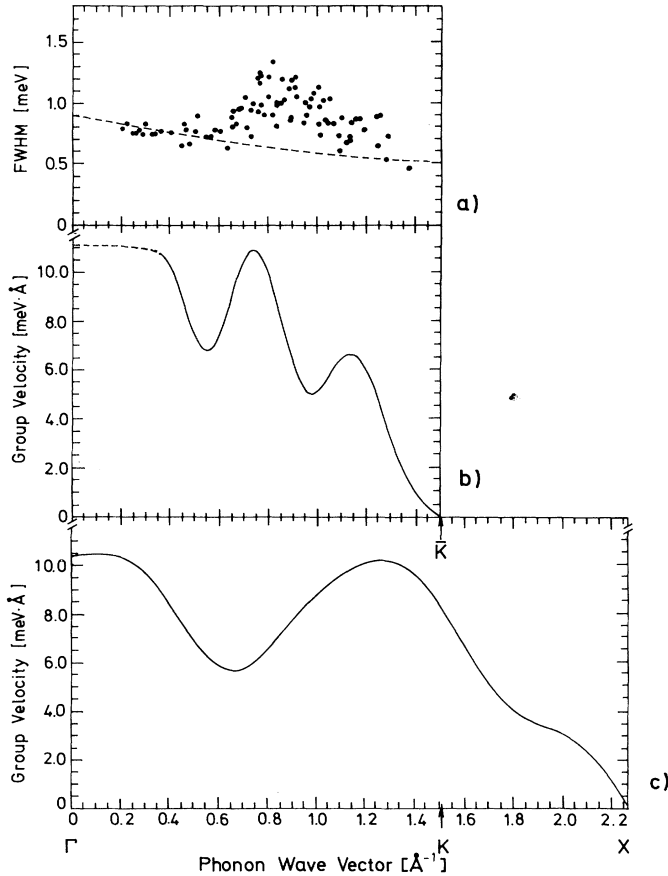


FIG. 3. Comparison of results for the surface and bulk group velocities. (a) The measured half-widths of the Rayleigh dispersion curve along $\langle 1\bar{1}0 \rangle$ for $T=160$ K derived from a single-Gaussian-distribution fit. (b) The Rayleigh-mode group velocity as a function of phonon wave vector calculated from the best-fit Fourier expansion. (c) The T_1 bulk group velocity calculated from the best-fit Fourier expansion of the data presented in Ref. 2.

a single-Gaussian-distribution fit. The half-widths show a distinct maximum at about $Q=0.8 \text{ \AA}^{-1}$. Half-widths obtained from a fit including a second Gaussian distribution for the second mode showed nearly the same behavior. Also the widths of the second-mode peaks were broadened at about 0.8 \AA^{-1} . For comparison the dashed line shows the calculated half-widths obtained from a full Monte Carlo simulation of the apparatus, which in previous work on Cu, Ag, and Au agreed well with the measurements. Thus the experiments show a strong broadening suggesting a coupling-induced decrease in phonon lifetime peaked at $Q=0.8 \text{ \AA}^{-1}$. The group velocity in Fig. 3(b) shows several features which are much sharper than in the bulk shown in Fig. 3(c). Since the anomalies may lead to maxima or minima in the group velocity¹ the assignment of these structures is not unambiguous. Because of the coincidence with the half-widths we assign the maxima at $Q=0.8$ and 1.2 \AA^{-1} as the probable positions of the anomalies. There are several possible theoretical locations of the anomaly in the bulk as estimated in Ref. 2, and the experiments do not show a clear preference. Calculations of generalized susceptibility $\chi(q)$ ¹⁵ do, however, predict the bulk anomaly to be at $q=0.55$ and 0.65 \AA^{-1} .

Increasing the surface temperature to 400 K resulted in a significant weakening of the anomaly, comparable to the temperature dependence of the bulk Kohn anomaly as reported in Ref. 2. This is expected since the sharpness of the anomaly is related to the existence of a well-defined Fermi surface which is smeared out at elevated temperatures.¹⁶ Additional evidence for the interpretation of our results in terms of a surface Kohn anomaly comes from measurements on a hydrogen-covered Pt(111)+H(1 \times 1) surface. Here the time-of-flight spectra show only the Rayleigh mode, which is reduced in frequency above $Q=0.6 \text{ \AA}^{-1}$, but do not

show a distinct anomaly in the dispersion curve. This is consistent with the possibility that the anomaly on the clean surface is due to an electronic surface state, which is severely affected by the adsorbate.

An alternative explanation is suggested by our previous results on Au(111) phonons, which show a sharp discontinuity at $Q = 0.85 \text{ \AA}^{-1}$ in the lowest-frequency dispersion curve. This has been attributed to a complicated hybridization of the pseudo Rayleigh mode with the Rayleigh wave and the longitudinal mode, the coupling being enhanced by the extreme (30%) softening of the longitudinal forces in Au.¹⁷ We do not feel that this occurs on Pt since the longitudinal and Rayleigh modes show relative frequencies more characteristic of Cu and Ag, where such discontinuities are not observed.

Because of the lack of measured or calculated electronic surface states on Pt(111) we cannot at the present time provide a definite assignment of the observed surface-phonon anomaly. Because of the significant shift in Q of the main surface anomaly to 0.8 \AA^{-1} with respect to the bulk anomaly at 0.6 \AA^{-1} we do not feel that the observed anomaly is a direct projection of the bulk anomaly onto the surface. Rather it appears to be a true two-dimensional anomaly, which shows the expected narrowing, compared to three dimensions. According to a theoretical study on TiN by Benedek *et al.*,¹⁸ the surface anomalies may be shifted to different Q values than in the bulk because of the reduced number of nearest and next-nearest neighbors at the surface. Our preferred explanation is that at $Q = 0.8$ and possibly at $Q = 1.2 \text{ \AA}^{-1}$ there is a strong coupling to surface electronic states. It is interesting to note that the reconstruction seen on the Pt(001) surface may be associated with a soft-phonon instability at $Q = 0.9 \text{ \AA}^{-1}$ in the Rayleigh mode, also in the $\langle 110 \rangle$ direction.⁸

We gratefully acknowledge discussions with B. Feuerbacher on experimental techniques. We

greatly profited from several extensive discussions with G. Benedek, V. Bortolani, and V. Celli. Finally, we thank G. Farnell for calculating the continuum-limit Rayleigh-phonon velocity, and D. Smilgies for simulating the time-of-flight peak widths.

¹W. Kohn, Phys. Rev. Lett. **2**, 393 (1959); E. J. Woll, Jr., and W. Kohn, Phys. Rev. **126**, 1693 (1962).

²D. H. Dutton, B. N. Brockhouse, and A. P. Miller, Can. J. Phys. **50**, 2915 (1972).

³A. M. Afanas'ev and Yu. Kagan, Zh. Eksp. Teor. Fiz. **43**, 1456 (1962) [Sov. Phys. JETP **16**, 1030 (1963)].

⁴M. J. Rice and S. Strässler, Solid State Commun. **13**, 125 (1973).

⁵N. Wakabayashi, H. G. Smith, and R. Shanks, Phys. Lett. **50A**, 367 (1974).

⁶S. E. Trullinger and S. L. Cunningham, Phys. Rev. Lett. **30**, 913 (1973), and Phys. Rev. B **8**, 2622 (1973).

⁷J. E. Inglesfield, J. Phys. C **12**, 149 (1979).

⁸J. G. Sanz and G. Armand, Surf. Sci. **118**, 291 (1982).

⁹E. Tasatti, Solid State Commun. **25**, 637 (1978).

¹⁰R. B. Doak, U. Harten, and J. P. Toennies, Phys. Rev. Lett. **51**, 578 (1983).

¹¹U. Harten, J. P. Toennies, and Ch. Wöll, Trans. Faraday Soc. (to be published).

¹²V. Bortolani, A. Franchini, F. Nizzoli, and G. Santoro, Phys. Rev. Lett. **52**, 429 (1984).

¹³G. W. Farnell, private communication.

¹⁴J. E. Black, F. C. Shanes, and R. F. Wallis, Surf. Sci. **133**, 199 (1983).

¹⁵A. J. Freeman, T. J. Watson-Yang, and J. Rath, J. Magn. Magn. Mater. **12**, 140 (1979).

¹⁶T. M. Rice and B. I. Halperin, Phys. Rev. B **1**, 509 (1970).

¹⁷V. Bortolani, G. Santoro, U. Harten, and J. P. Toennies, Surf. Sci. **148**, 82 (1984).

¹⁸G. Benedek, M. Miura, W. Kress, and H. Bilz, Phys. Rev. Lett. **52**, 1907 (1984).